EXPERIMENTAL STUDY ON ADIABATIC TWO-PHASE EXPANSION IN A CYLINDER FOR TRILATERAL CYCLE

H. Kanno[1,2]*, Y. Hasegawa[2], I. Hayase[2] and N. Shikazono[2]
[1] Railway Technical Research Institute, Drive systems, Vehicle control Technology Division,
2-8-38 Hikari-cho, Kokubunji-shi,Tokyo, Japan
E-mail: kanno.hiroshi.14@rtri.or.jp

[2] Institute of Industrial Science, The University of Tokyo,
4-6-1 Komaba, Meguro-ku, Tokyo, Japan
E-mail: shika@iis.u-tokyo.ac.jp

* Corresponding Author

ABSTRACT

In the present study, temperature and pressure measurements and visualization of two-phase adiabatic expansion for trilateral cycle are carried out. Experimental setup with piston and cylinder which mimics the reciprocating expander is constructed and boiling phenomenon is visualized. Working fluids are water and ethanol, and initial temperatures are 100 and 80 ℃ in this study. Output work is calculated from the $P - V$ diagram. In addition, filter-type sintered metal is fixed on the bottom of the cylinder to enhance boiling. The difference between measured and quasi-static pressures becomes larger and the adiabatic efficiency decreases as piston velocity is increased. With sintered metal filter on the bottom of the cylinder, the deterioration of adiabatic efficiency becomes moderate for both working fluids because of the initial captured bubbles in the sintered metal. The adiabatic efficiency for pore diameter of d_{pore} = 20 μm and piston velocity 300 mm/s case is about 87 % for water, which is 1.05 times larger than that of the smooth surface condition. For ethanol, the adiabatic efficiency was about 92 % which is 1.18 times larger than that of the smooth surface condition. To investigate the feasibility of the two-phase expander, an experiment reproducing the intake and exhaust processes is conducted. The adiabatic efficiency increases with the increase of maximum piston velocity because of the reduction of heat loss. The sintered metal filter for boiling enhancement is also effective in an expander with intake and exhaust processes.

1. INTRODUCTION

In recent years, trilateral cycle attracts large attentions for waste heat recovery from moderate or low temperature heat sources (Smith et al., 1993, 1994, 1996, Fischer, 2011, Steffen et al., 2013). In the trilateral cycle, working fluid is pressurized and kept as a single liquid phase during the heating process. Heat is transferred from the heat source to the single phase working fluid, so the exergy loss can be drastically reduced because of favorable temperature profile matching between the heat source and the working fluid. In the expansion process, working fluid is flashed and becomes liquid-vapor two-phase. Thus, for the trilateral cycle system, the heat exchanger to reduce temperature difference and the two-phase expander are the key components.

For two-phase expansion or wet-vapor expansion, Lysholm turbine, scroll or reciprocating expanders have been investigated from the view point of erosion durability. Smith et al. (1993, 1994 and 1996) estimated the performance and cost of trilateral flash cycle using Lysholm twin screw turbine. They reported that the adiabatic efficiency of the expander can reach 70 %, and that the trilateral flash cycle can produce 1.8 times larger output power than a simple Rankine cycle for hot steam of 100 – 200 ℃. Steffen et al. (2013) proposed a novel trilateral cycle using cyclone separator and reciprocating

expander, and simulated the influence of injection timing, material of cyclone, the size and frequency of reciprocating expander. They concluded that the effective thermal insulation of the cyclone wall is important, and found that large stroke volume and engine speed deteriorate isentropic efficiency of the expander due to the influence of injection timing. Bao et al. (2013) reviewed the advantages of several kinds of expanders from the view point of the working fluid, capacity and cost. They reported that reciprocating piston expander has the advantage of adaptability for variable working conditions and tolerance for two-phase expansion.

A two-phase expansion in adiabatic condition in constant volume chamber is called as flash evaporation. Yan et al. (2010) and Zhang et al. (2012) conducted an experimental study on static and circulatory flash evaporation, and investigated the steam-carrying effect. Saury et al. (2005) studied flash evaporation of water film and proposed a correlation between the dimensionless maximum mass flow rate, dimensionless initial temperature, depressurization rate, superheat and initial water height.

The above flash evaporation studies were carried out in a flash chamber, but did not focus on the output work which could be taken out from the system. Therefore, research on adiabatic two-phase expansion to generate output power or enhancing boiling in an expander is not fully investigated. As mentioned by Bao et al. (2013), reciprocating expander has several advantages for the two-phase expansion. However, experimental study for reciprocating two-phase expansion is still limited.

In this study, working fluid is expanded in a thermally insulated cylinder and boiling is visualized by the high speed micro scope to investigate the basic characteristics of adiabatic two-phase expansion in a reciprocating expander. The working fluid and the setup are warmed up before the expansion experiment to exclude the effect of heat loss. The pressure sensor and thermo-couple are embedded in the piston to measure vapor temperature. The output power is obtained from the measured $P - V$ diagram. The effect of piston velocity on adiabatic efficiency is evaluated. In addition, sintered metal filter is placed on the bottom of the cylinder to enhance boiling. To investigate the feasibility of the two-phase expander, continuous reciprocating expansion experiment is conducted. The adiabatic efficiency and heat loss are investigated and the effectiveness of the sintered metal is also evaluated.

2. TWO-PHASE EXPANSION EXPERIMENT

2.1 Experimental setup and procedure

Figure 1 shows the insulated cylinder for two-phase expansion experiment. In this study, water of 100 ℃ and ethanol of 80 ℃ are used as the working fluids. The cylinder is a double pipe made of polycarbonate. The piston with diameter of D_p = 55 mm is also made of polycarbonate. The bottom of the cylinder is made of thin stainless plate with thickness of 0.8 mm. The working fluid and the setup are heated up to the operating temperature by hot air in order to exclude the effect of heat loss. Then, the double tube and the back side of the cylinder bottom are vacuumed by a vacuum pump for thermal insulation before the expansion experiment. The temperatures of liquid and vapor phases are measured by the thermo-couples attached to the piston and the bottom of the cylinder. The pressure in the cylinder is measured by the pressure sensor embedded in the piston. Indicated work is obtained from a P - V diagram.

Figure 2 shows the schematic of the experimental setup. Table 1 shows the physical properties of the stainless plate and the cylinder. Table 2 shows the experimental condition. The two-phase expansion experiments are carried out in the following procedure. First, the piston is initially set at $z_p = z_0$ by the linear actuator (EZC6D030M-K, Oriental Motor). Then, by operating the cross valves No.4, 5 and 6, the hot air from the heater (SD-2-2, Sakaguchi E.H VOC) is introduced to the insulation chamber (double-pipe cylinder) to warm up the setup. During this procedure, the flash chamber (test section) is connected to the vacuum pump (GLD-201B, Ulvac) by switching the cross valve 7 to purge the air in the test section. When the pressure in the test section becomes smaller than 0.001 MPa, the cross valves No. 7 and 8 are switched, and then the test section is connected to the syringe (1050-TLL, GL

Science). After the working fluid of m_0 is introduced to the test section from the syringe, cross valve No. 7 is switched to isolate the test section. During and after these procedures, hot air is introduced to the insulation chamber to heat the working fluid and the cylinder walls. The temperature of hot air is controlled by the heat regulator (E5CB-Q1TC, Omron) and the solid state relay (G3PA-210B-VDDC5-24, Omron). When the liquid temperature T_{liq} reaches initial operating temperature T_0, hot air supply is stopped by switching the cross valve No. 4. Then, the cross valves No.5 and 6 are switched immediately and remained hot air is withdrawn to the vacuum pump. In this procedure, the setup is thermally insulated by vacuum insulation. Then, the piston is moved by the linear actuator motor firstly with a constant acceleration of α_p, and then with constant velocity of $v_{p,max}$, and finally decelerated with α_p.

The pressure inside the cylinder is measured by the pressure sensor (PHS-B-200KP, Kyowa), and its signal is amplified by the dynamic strain amplifier (DMP911B, Kyowa). The temperatures of liquid and vapor phases are measured by sheath-type thermocouples (1HKN033, Chino) with outer diameter of 0.3 mm. The piston displacement is observed by the pulse counter (CNT-3921-E-DF, Coco Research). All analog data are recorded on the midi-logger (GL7000, Graphtec) with the sampling frequency of 10 msec. Boiling phenomenon is visualized by the high speed micro scope (VW-9000, Keyence) with the frame speed of 1000 fps.

Sintered metal filter to enhance boiling is placed on the bottom of the cylinder by silicone-type adhesion bond. Table 3 shows the properties of sintered metal filter.

The adiabatic efficiency η_{ad} is defined as the ratio of the measured indicated work to that of the quasi-static expansion, as shown in Eqs. (1), (2) and (3). The quasi-static pressure change p'_{ise} is calculated assuming isentropic expansion by using REFPROP ver. 9.0 (2010). In this study, the total transferred heat (the effect of heat loss) is taken into account when calculating the quasi-static work. If the piston velocity is very slow, i.e. $v_{p,max}$ = 1or 2 mm/s, the effect of heat loss on the adiabatic efficiency cannot be neglected. The amount of heat loss is obtained by measuring the liquid temperature during the calibration experiment. Figure 3 shows the liquid temperature change for water. From the temperature change measured in this calibration experiment, heat rate (heat loss) from the setup to the atmosphere is obtained and the corrected quasi-static pressure is calculated.

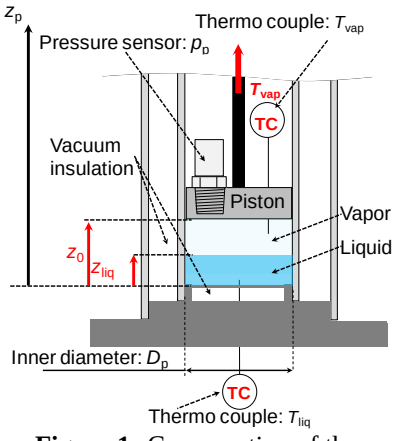

Figure 1: Cross section of the cylinder and the piston.

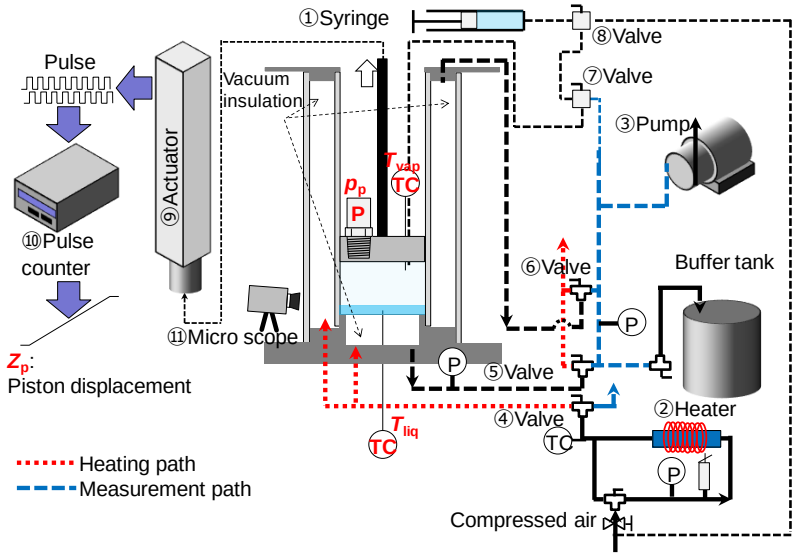

Figure 2: Schematic of the experimental setup

Table 1: Physical properties of stainless plate and cylinder

	Stainless plate (SUS304)	Cylinder (polycarbonate)
ρ (kg/m^3)	9790	1200
C (kJ/kgK)	0.59	1.05

Table 2: Experimental condition

Parameter	Value
z_{liq} (mm)	6
z_0 (mm)	9
ε_{exp}	20
α_p (mm/s^2)	833
$v_{p,max}$ (mm/s)	1 – 300

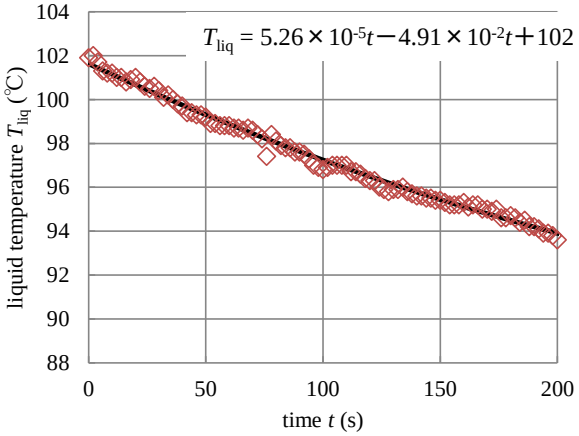

Figure 3: Liquid temperature change for water, 100 ℃.

Table 3: Properties of sintered metal filter

Material	Pore diameter (μm)	Porosity (%)	Thickness (μm)
SUS304	5	80	0.37
	20	79	0.62
	75	87	0.87

$$\eta_{ad} = \frac{W_{exp}}{W'_{ise}} \tag{1}$$

$$W_{exp} = \int p_p \mathrm{d}V_{cyl} \tag{2}$$

$$W'_{ise} = \int p'_{ise} \mathrm{d}V_{cyl} \tag{3}$$

2.3 Experimental Results

Figure 4 and Figure 5 show the visualization results with smooth surface for water and ethanol, respectively. Boiling bubbles are observed from the edge of the bottom of the cylinder. The number and frequency of the boiling bubbles increase as the piston velocity is increased in both working fluids. Figure 6 shows the visualization for water with sintered metal filter of d_{pore} = 20 μm. The number of bubbles increased compared with the smooth surface case. The density of bubble departure sites also increased. Figure 7 shows the visualization for ethanol with sintered metal filter of d_{pore} = 20 μm. A lot of small bubbles are generated from the sintered metal filter, and the vapor-liquid interface is lifted by the bubbles. For both cases, boiling is enhanced by using sintered metal filter. In this experiment, the working fluid is heated from the bottom of the cylinder before the expansion process, and boiling bubbles are observed from the sintered metal during this heating process. It is considered that the small bubbles trapped by the sintered metal filter are the initial boiling sites. The small bubbles remained in the sintered metal filter before the expansion process are effective to enhance boiling in adiabatic expansion.

Figure 8 shows the P – V diagram for water with piston speed of $v_{p,max}$ = 128 mm/s. The pressure decreases immediately and the pressure reduction becomes moderate afterwards. During the expansion process, the pressure becomes high with sintered metal filter compared with the smooth surface case. The pressure is generally higher for the sintered metal filter with larger pore diameters. Figure 9 shows the adiabatic efficiencies for water. Adiabatic efficiency decreases as the piston velocity is increased, while the efficiency becomes higher for larger pore diameters. In the case of $v_{p,max}$ = 300 mm/s and d_{pore} = 20 μm, the adiabatic efficiency is about 87 % which is 1.05 times larger than that of the smooth surface case. In general, wettability of water is poor and the bubble diameter

observed in the visualization is larger than that of ethanol. Therefore, boiling is more enhanced when using large pore diameter filters.

Figure 10 shows the $P - V$ diagram for water with piston speed of $v_{p,max}$ = 128 mm/s. The pressure reduction is restrained by the effect of boiling enhancement when using the sintered metal filter of d_{pore} = 5 and 20 mm. For d_{pore} = 75, boiling becomes unstable. In some cases, pressure is kept high, but in other cases, the pressure decreases immediately and recovers by following explosive boiling. Figure 11 shows the adiabatic efficiencies for ethanol. For $v_{p,max}$ = 300 mm/s and d_{pore} = 20 μm case, the adiabatic efficiency is about 92 % which is 1.18 times larger than that of the smooth surface case. When using the sintered metal filter of d_{pore} = 75, the adiabatic efficiency value varies due to the unstable boiling. For ethanol, wettability is better than water, and it is difficult to keep the initial nucleate bubble until the expansion process starts. From these results, it is considered that small pore diameter is preferable when using working fluids of good wettability.

Figure 4: Visualization for water with smooth surface. (a) $v_{p,max}$ = 8 mm/s, (b) $v_{p,max}$ = 32 mm/s and (c) $v_{p,max}$ = 128 mm/s.

Figure 5: Visualization for ethanol with smooth surface. (a) $v_{p,max}$ = 8 mm/s, (b) $v_{p,max}$ = 32 mm/s and (c) $v_{p,max}$ = 128 mm/s.

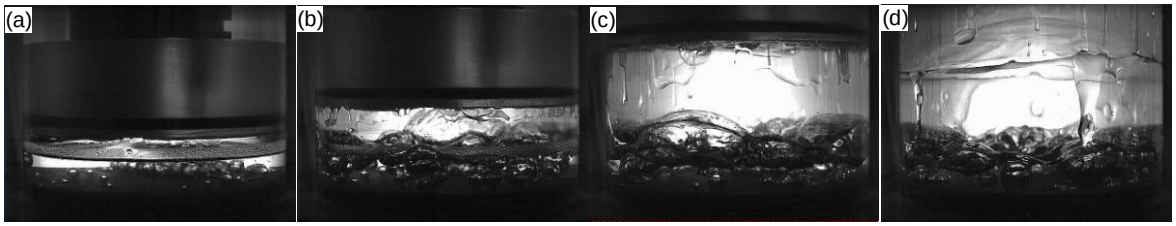

Figure 6: Visualization results for water with sintered metal filter of d_{pore} = 20 μm and $v_{p,max}$ = 128 mm/s. (a) t = 0.05, (b) t = 0.1, (c) t = 0.2, and (d) t = 0.4.

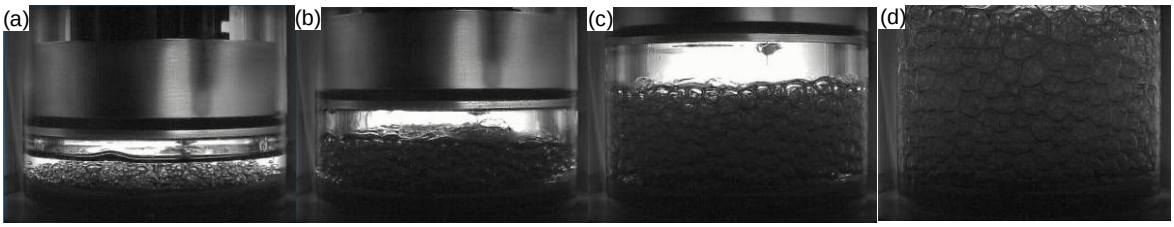

Figure 7: Visualization results for ethanol with sintered metal filter of d_{pore} = 20 μm and $v_{p,max}$ = 128 mm/s. (a) t = 0.05, (b) t = 0.1, (c) t = 0.2, and (d) t = 0.4.

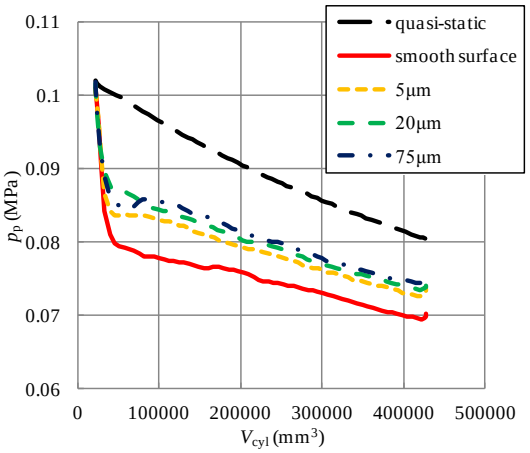

Figure 8: *P – V* diagram for water and $v_{p,max}$ = 128 mm/s.

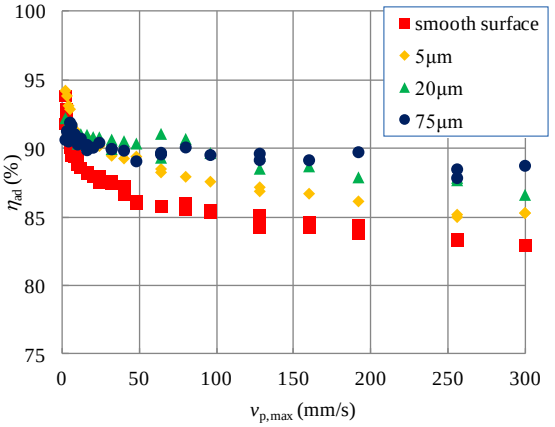

Figure 9: Adiabatic efficiencies for water.

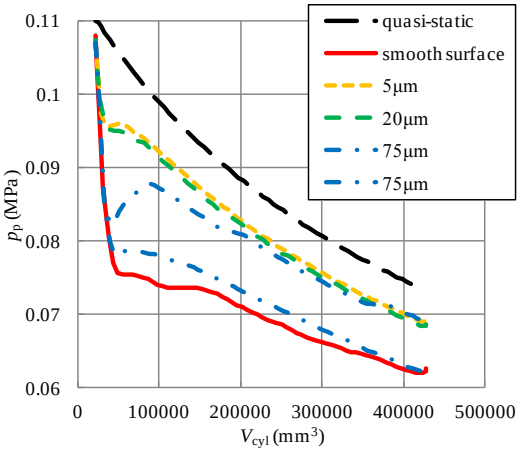

Figure 10: *P – V* diagram for ethanol and $v_{p,max}$ = 128 mm/s.

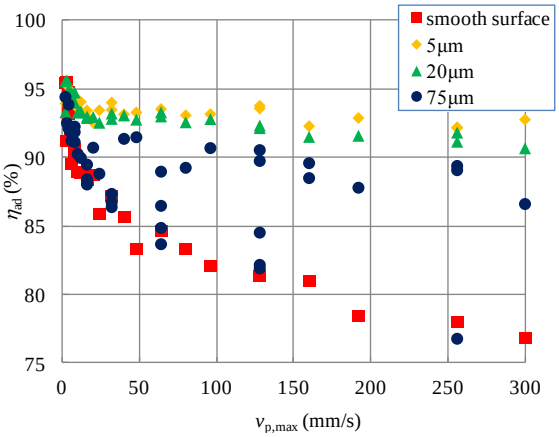

Figure 11: Adiabatic efficiencies for ethanol.

3. TWO-PHASE EXPANSION IN RECIPROCATING EXPERIMENTAL SETUP

3.1 Experimental setup and procedure

In the actual reciprocating expander, expansion process is divided into three processes, i.e. intake, expansion and exhaust. In the intake process, hot working fluid is introduced into the cold cylinder, so the heat loss deteriorates the adiabatic expansion, while the initial bubbles in the cylinder can enhance boiling.

Figure 12 shows the reciprocating experimental setup. The piston, cylinder and the mechanism of setup-warming and vacuum insulation are the same as the previous setup, while a mechanism to introduce hot working fluid into the cylinder is added. Water of 100 ℃ and ethanol of 80 ℃ are used as the working fluids. Working fluid in supply-tank No.1, pre-heater No.2, and heater No.4 is heated to the operating temperature T_0. At the beginning of the expansion process, the heated working fluid is introduced by the plunger No. 3 pushed by the actuator No.11. The working fluid introduced into the cylinder No.5 is expanded by the piston moved by the actuator No.11. At the beginning of exhaust process, the exhaust valve is opened by DC solenoid and the working fluid in the cylinder is exhausted to the vacuum tank No.6. The back pressure in the vacuum tank is kept about 0.02 MPa.

In this experiment, the piston and the plunger for introducing the working fluid are accelerated and decelerated respectively. The cut-off timing which is the timing to stop introducing the working fluid is determined by the plunger displacement. Figure 13 shows the cut-off timing. The cut-off volume ratio $\varepsilon_{cut,vol}$ is defined by Eq. (4), and the expansion ratio ε_{exp} is defined by Eq. (5). Table 4 shows the experimental condition. The maximum piston velocity is changed by acceleration α_p. Note that the

acceleration is fixed as α_p = 96 mm/s^2 in the warming-up operation.

Warming-up operation including 10 cycles of intake, expansion and exhaust processes is conducted. After this warming-up operation, data during 5 cycles of intake, expansion and exhaust processes are collected. Figure 14 shows the example of warming-up operation and data acquisition operation. Liquid temperature T_{nozzle} measured in the inlet nozzle is gradually increased in the warming-up operation and kept at the operating temperature within the range of about ± 2 ℃ during the data acquisition operation. Output work is calculated by taking the average of 5 cycles of the $P - V$ diagram, and adiabatic efficiency is evaluated.

In this experiment, the initial temperature of the bottom plate before the expansion process is assumed to be the same as the saturated temperature of p_p before the expansion. Then, heat loss E_{loss} from the working fluid to the bottom plate is calculated. The isentropic efficiency which excludes the effect of the heat loss is defined as Eq. (6).

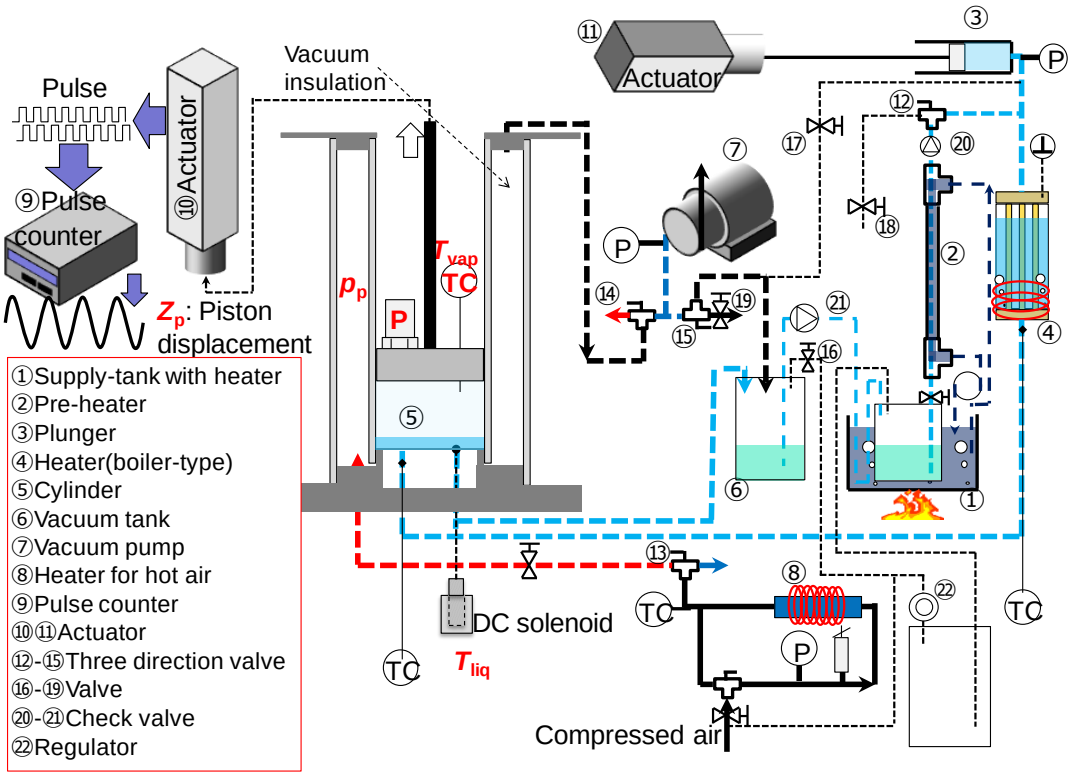

Figure 12: Schematic of the reciprocating experimental setup

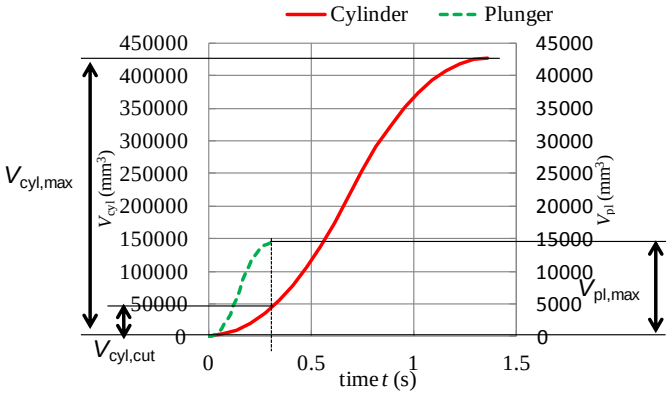

Figure 13: Cut-off point

Table 4: Experimental condition

Parameter	Value
z_{liq} (mm)	6
z_0 (mm)	0.5
z_{max} (mm)	180
α_p (mm/s^2)	10 - 769
$v_{p,max}$ (mm/s)	42.4 – 371.6
$\varepsilon_{cut,vol}$ (mm/s)	3
ε_{exp} (mm/s)	30

In warming-up operation, α_p is 96.2.

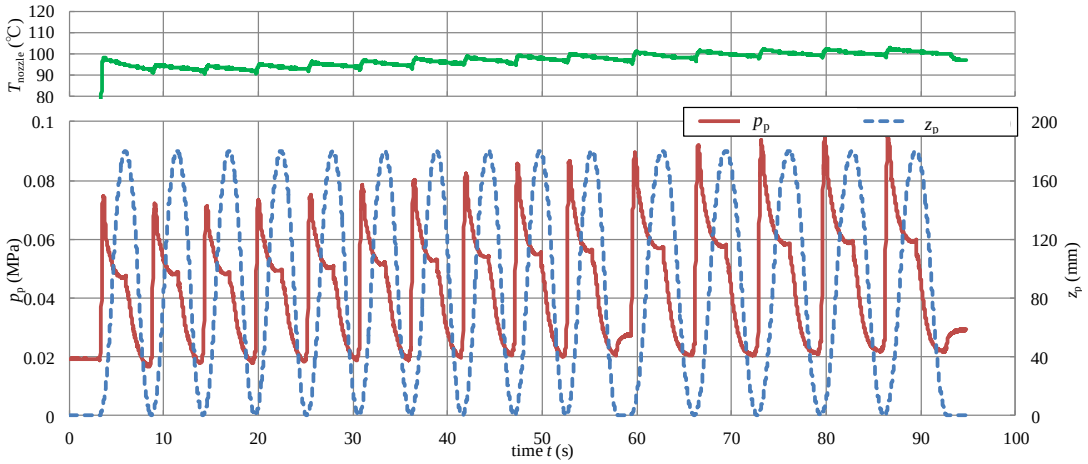

Figure 14: 10 cycles of warming-up operation and 5 data acquisition cycles for water at α_p = 47.8 mm/s^2.

$$\varepsilon_{\text{cut,vol}} = \frac{V_{\text{cyl,cut}}}{V_{\text{pl,max}}} \tag{4}$$

$$\varepsilon_{\text{exp}} = \frac{V_{\text{cyl,max}}}{V_{\text{pl,max}}} \tag{5}$$

$$\eta_{\text{ise}} = \frac{W_{\text{exp}}}{W_{\text{ise}} - E_{\text{loss}}} \tag{6}$$

3.2 Experimental results

Figure 15 shows the efficiencies with smooth surface and sintered metal filter of d_{pore} = 20 μm for water as a working fluid. The isentropic efficiency decreases or remains nearly constant with the increase of piston velocity, while the adiabatic efficiency increases because of the reduction of heat loss. It can be considered that the effect of heat loss becomes negligible when the piston velocity is high. When using the sintered metal filter, the adiabatic efficiency increases. However, the effect of the sintered metal filter becomes small as the piston velocity is increased.

Figure 16 shows the efficiencies for ethanol with smooth surface and sintered metal filter of d_{pore} = 20 μm. The adiabatic efficiency of the sintered metal filter is about 5 % higher than that of the smooth surface case. From these results, the boiling enhancement is also important for the reciprocating expander with intake and exhaust processes, and the sintered metal filter should be also effective.

Ohman et al. (2013) reported that the adiabatic efficiency for vapor expansion in a Lyshol turbine is about 60 – 80 %, and it slightly decreases as the vapor quality measured at the inlet of the expander is reduced. Their study takes into account the electrical loss of generator and leakage loss to obtain adiabatic efficiency. In our reciprocating experiment, the maximum value of adiabatic efficiency is about 85 %, while the efficiency is defined by the indicated work. Therefore, if the mechanical and electrical losses are taken into account, the adiabatic efficiency should decrease a little from this value. From these results, the adiabatic efficiency of two-phase expansion can achieve nearly the same efficiency as the vapor expansion used for Rankine cycle. It is noted that the exergy efficiency of trilateral cycle is higher than that of Rankine cycle if the expander efficiencies are the same, which is shown by thermodynamic analysis in our previous study (Kanno et al., 2014).

For reciprocating expansion, several losses must be considered. For example, the injection loss due to the delay of the working fluid introduction, and non-equilibrium loss which is caused by the temperature difference between the liquid phase and vapor phase should be considered. To increase the adiabatic efficiency for high piston velocity conditions, reduction of non-equilibrium loss is important. Further investigation is required for understanding non- equilibrium loss.

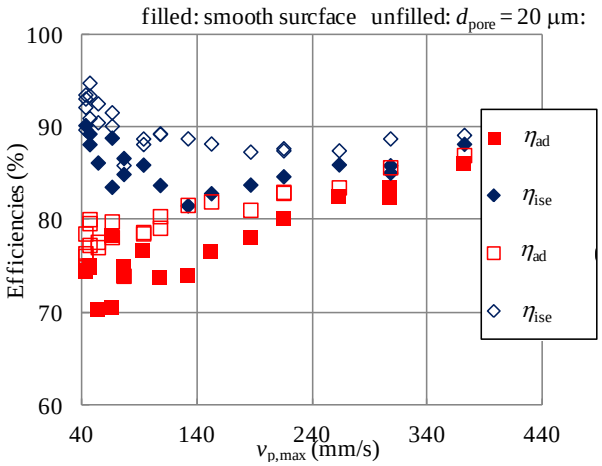

Figure 15: Efficiencies for water.

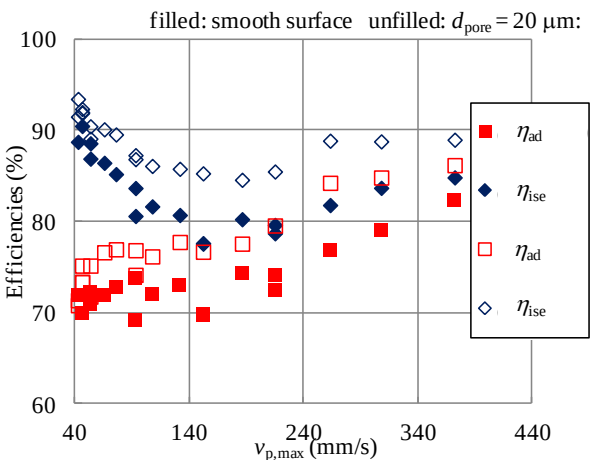

Figure 16: Efficiencies for ethanol.

4. CONCLUSIONS

An adiabatic two-phase expansion experiment in a cylinder with moving piston is conducted. From the experimental results, following conclusions are obtained.

When the heat loss is excluded, the adiabatic efficiency decreases with piston velocity. Sintered metal filter fixed on the bottom of the cylinder can enhance boiling. The adiabatic efficiency for pore diameter of d_{pore} = 20 μm and piston velocity 300 mm/s is about 87 % for water, which is 1.05 times larger than that of smooth surface condition. The adiabatic efficiency is about 92 % for ethanol, which is 1.18 times larger than that of the smooth surface condition. In the actual reciprocating expander with intake, expansion and exhaust processes, the effect of heat loss to the setup cannot be neglected. However, the effect of heat loss decreases with the increase of the piston velocity. The sintered metal filter is also effective to enhance boiling for the reciprocating expanders with intake and exhaust processes. Reciprocating two-phase expander can achieve nearly the same adiabatic efficiency as the vapor expander. Thus, it is considered that trilateral cycle can achieve very high exergy efficiency as expected.

NOMENCLATURE

C	specific heat	(kJ/kgK)
D	diameter	(mm)
E	heat or energy	(J)
m	mass	(kg)
p	pressure	(MPa)
t	time	(s)
T	temperature	(℃)
v	velocity	(mm/s)
V	volume	(mm^3)
W	output work	(J)

Greek symbols

α	acceleration	(mm/s^2)
ε	volumetric ratio	(-)
η	efficiency	(%)
ρ	density	(kg/m^3)

Subscript

0	initial condition

ad	adiabatic
cut	cut-off
cyl	cylinder
exp	expansion
ise	isentropic
liq	liquid
loss	loss
max	maximum
nozzle	nozzle
p	piston
pl	plunger
pore	pore
vap	vapor
vol	volumetric

REFERENCES

Bao, J., Zhao, L., 2013, A review of working fluid and expander selections for organic Rankine cycle, *Renewable and sustainable Energy Reviews*, vol. 24, pp. 325 – 342.

Fischer, J., 2011, Comparison of trilateral cycles and organic Rankine cycles, *Energy* Vol. 36, pp. 6208 – 6219.

Kanno, H., Shikazono, N., 2014, Thermodynamic Simulations of Rankine, Trilateral and Supercritical Cycles for Hot Water and Exhaust Gas Heat Recovery, *Mechanical Engineering Journal*, Vol. 1 , p. TEP0046.

Lemmon, E.W., Huber, M.L., McLinden, M.O., 2010, NIST standard reference database 23: reference fluid thermodynamic and transport properties REFPROP version 9.0. Gaithersburg: *National Institute of Standards and Technology*, Standard Reference Data Program;.

Ohman, H., Lundqvist, P., 2013, Experimental investigation of a Lysholm Turbine operating with superheated, saturated and 2-phase inlet conditions, *Applied Thermal Engineering*, vol. 50, pp. 1211 – 1218.

Oreijah, M., Date, A., Akbarzadaha, A., 2014, Comparison between Rankine Cycle and Trilateral Cycle in Binary System for Power Generation, *Applied Mechanics and Materials*, vol. 464, pp. 151-155.

Saury, D., Harmand, S., Siroux, M., 2005, Flash evaporation from a water pool:Influence of the liquid height and of the depressurization rate, *International Journal of Thermal Sciences*, vol. 44, pp. 953–965.

Smith, I.K., 1993, Development of the trilateral flash cycle system. 1. Fundamental considerations., *Journal of Power and Energy*, vol. 207, pp. 179-194.

Smith, I.K., Dasilva, R.P.M., 1994, Development of the trilateral flash cycle system. 2. Increasing power output with working fluids mixtures, *Journal of Power and Energy*, vol. 208, pp. 135-144.

Smith, I.K., Stosic, N., Aldis, C.A., 1996, Development of the trilateral flash cycle system. 3. The design of high-efficiency two-phase screw ex panders, *Journal of Power and Energy*, vol. 210, pp. 75-93.

Steffen, M., Lofffler, M., Schaber, K., 2013, Efficiency of a new Triangle Cycle with flash evaporation in a piston engine, *Energy*, Vol.57, pp. 295-307.

Yan, J., Zhang, D., Chong, D., Wang, G., Li, L., 2010, Experimental study on static/circulatory flash evaporation, *International Journal of Heat and Mass Transfer*, vol. 53, pp. 5528–5535.

Zhang, D., Chong, D., Yan, J., Zhang, Y., 2012, Study on steam-carrying effect in static flash evaporation, *International Journal of Heat and Mass Transfer*, vol. 55, pp. 4487–4497.

ACKNOWLEDGEMENT

This work has been partly supported by the Japan Science and Technology Agency (JST). The authors gratefully acknowledge for the financial support.